BMP1 inhibitor UK-383,367 attenuates renal fibrosis and inflammation in CKD

Mi Bai [1,2,3 *], Juan Lei[1,2 *], Shuqin Wang[1,2], Dan Ding [1,2], Xiaowen Yu[1,2,3], Yan Guo [1,2,3], Shuang Chen [1,2], Yang Du[1,2], Deyi Li[4], Yue Zhang [1,2], Songming Huang [1,2], Zhanjun Jia [1,2,3*], and Aihua Zhang[1,2,3*]

1. Department of Nephrology, State Key Laboratory of Reproductive Medicine, Children's Hospital of Nanjing Medical University, Nanjing, China

2. Jiangsu Key Laboratory of Pediatrics, Nanjing Medical University, Nanjing, China

3. Nanjing Key Lab of Pediatrics, Children's Hospital of Nanjing Medical University, China

4. School of Life Sciences and Biopharmaceutics, Shenyang Pharmaceutical University, Shenyang, China

* M Bai and J Lei contributed equally to this work.

*Z Jia and A Zhang contributed equally to this work.

Correspondence to: Aihua Zhang, M.D., Ph.D., Department of Nephrology, Nanjing Children's Hospital, Affiliated to Nanjing Medical University, 72 Guangzhou Road, Nanjing 210008, P. R. of China, Tel: 0086-25-8311-7309, Fax: 0086-25-8330-4239, Email: zhaihua@njmu.edu.cn.

Running tittle: BMP1 inhibitor attenuates renal fibrosis

Abstract

Renal fibrosis is a key pathological phenomenon of chronic kidney disease (CKD), contributing to the progressive loss of renal function. UK383,367 is a procollagen C-proteinase inhibitor that has been selected as a candidate for dermal anti-scarring agent, while its role in renal fibrosis is unclear. In this study, UK383,367 was applied to a CKD mouse model of unilateral ureteral obstruction (UUO) and cell lines of renal tubular epithelial cells (mPTCs) and renal fibroblast cells (NRK-49F) challenged by TGF-β1. In vivo, bone morphogenetic protein 1 (BMP1), the target of UK383,367, was significantly enhanced in UUO mouse kidneys and CKD patients' renal biopsies. Strikingly, UK383,367 administration ameliorates tubulointerstitial fibrosis shown by Masson's trichrome staining in line with the blocked expression of collagen I/III, fibronectin, and α-SMA in the kidneys from UUO mice. Similarly, the enhanced inflammatory factors in obstructive kidneys were also blunted. In vitro, UK383,367 pretreatment inhibited the induction of collagen I/III, fibronectin, and α-SMA in both mPTCs and NRK-49F cells treated with TGF-β1. Taken together, these findings indicated that BMP1 inhibitor UK383,367 could serve as a potential drug in antagonizing CKD renal fibrosis by acting on the maturation and deposition of collagen and subsequent profibrotic response and inflammation.

Key words: CKD, renal fibrosis, BMP1, UK383,367, inflammation

Introduction

Chronic kidney disease (CKD) has shown epidemic characteristics high morbidity and mortality (3, 14). Currently, we have no satisfactory strategies to delay or prevent the progression of CKD to end-stage renal disease (ESRD). Once CKD progresses to ESRD, patients must rely on renal replacement therapies, such as hemodialysis, peritoneal dialysis, or kidney transplantation. Therefore, to develop a new therapy to effectively deal with CKD is an urgent task. Renal fibrosis is a common pathology contributing to the development of chronic renal disease (CKD) and its progression to ESRD(21). Pathological phenotypes of fibrotic kidney include glomerulosclerosis, tubulointerstitial fibrosis, inflammatory cell infiltration, and renal parenchyma loss (tubuloatrophy, capillary occlusion, and podocyte loss)(22). A number of studies have shown that renal interstitial fibrosis is resulted from the aggregation and activation of renal myofibroblast, producing excessive extracellular matrix (ECM) components including collagen I, collagen III, and fibronectin(4, 17). Thus, directly targeting the ECM components could be a promising strategy in treating renal fibrosis and CKD.

Bone morphogenetic protein 1 (BMP1), also known as procollagen C-proteinase(19), belongs to the peptidase M12A family of bone morphogenetic protein (BMP), which induces bone and cartilage development. Unlike other BMPs, BMP1 does not belong to the TGF-β superfamily. It has the property of metal protease (Matrix Metalloproteinases, MMPs) cutting the C terminal of pre collagen I, II, and III, leading to the maturation of collagens and the deposition of ECM (7, 10, 12, 15).

Grgurevic, L. et al reported that BMP1 promotes the cleavage of type I procollagen, resulting in collagen deposition in cirrhosis (8). In addition, it is also reported that in the rat model of chronic kidney disease, BMP1-3 (BMP1 splicing subtype) can promote renal fibrosis by increasing ECM deposition which was attenuated by specific polyclonal antibody against BMP1-3 (9). Above reports suggested a potential of BMP1 antagonism in treating CKD renal fibrosis.

UK-383,367 is a procollagen C-proteinase (BMP1) inhibitor and is becoming a promising drug in treating dermal scarring (6). By now, no studies were reported to show the effect of UK383,367 on renal fibrosis in CKD. In the present study, employing the mouse CKD model (UUO) and kidney cells, we evaluated the role of UK383,367 in renal fibrosis to explore new potential of CKD therapy.

MATERIALS AND METHODS

Reagents and antibodies. DMEM/F12 medium and fetal bovine serum (FBS) were purchased from GIBCO. UK-383,367 was purchased from Selleck (Shanghai, China). CCK8 kit was purchased from MCE (MedChemExpress) China. Antibodies against FN1, CollagenI, CollagenIII, α-SMA and BMP1 were purchased from Abcam (Cambridge, MA). Anti-GAPDH antibody was from Santa Cruz Biotechnology (SantaCruz, CA). IL-1β ELISA kit was purchased from Novus Biological (Littleton, USA).

Patients. Renal biopsy samples were obtained from CKD patients who were undergoing diagnostic evaluation at the Department of Nephrology, Children's

Hospital of Nanjing Medical University. Renal biopsy samples were collected based on the criterion of having at least ten glomeruli in a paraffin-embedded tissue sample available for histological sectioning. A total of 8 subjects (age range 2-11 years old) were enrolled and pathologically diagnosed with diffuse interstitial nephritis (DIN), focal segmental glomerulosclerosis (FSGS), sclerosing glomerulonephritis or IgA nephropathy. The patient information was listed in Table 1. Normal renal tissues were collected from patients without proteinuria who received a partial nephrectomy of a benign renal tumor.

The protocol for the use of biopsied samples and nephrectomized tissues from patients was approved by the local committee on human subjects at Children's Hospital of Nanjing Medical University. Written informed consent was provided by each patient.

Establishment of mouse UUO model. In unilateral ureteral obstruction (UUO) experiment, 8-wk-old C57BL/6J male mice, weighing 25-30g, following anesthesia, the left ureter was ligated at the ureteropelvic junction with a 4-0 silk suture through a left flank incision. UK-383,367 was dissolved in 15% w/v hydroxypropyl-β cyclodextrin to a working concentration of 0.4μg/μl before injection and were intraperitoneally delivered to mice at 5 mg/kg/d. UK-383,367 or control injections were given at -1 to 7days after UUO surgery. Mice were sacrificed after 7 days of UUO and kidney samples were harvested for analyses. Animal work was performed in the Animal Core Facility at Nanjing Medical University. All animal studies were approved by the Nanjing Medical University Institutional Animal Care and Use Committee.

Cell culture studies. mPTCs and NRK-49F were grown in serum-free keratinocyte medium supplemented with bovine pituitary extract and epidermal growth factor (Wisent). The cells were specifically grown at 37°C with 5% CO_2 and subcultured at 50-80% confluence using 0.25% trypsin-0.02% EDTA (Invitrogen). In certain experiments, the cells were pre-treated with UK-383,367 (100nM or 200nM) for half an hour or transfected with BMP1 plasmids for 24 h, then treated with recombinant human TGF-β1 (10 ng/ml).

Quantitative real-time PCR. Total RNA was extracted from tissues or cells using the TRIzol (Invitrogen, Carlsbad, CA) according to the manufacturer's instructions. 500 nanogram of total RNA from each sample was used. cDNA was reverse transcribed according to the instructions of the Takara kit. The target gene and reference gene were amplified by quantitative real-time PCR. Cycle threshold values were used to calculate the relative amount of sample template. The 20μl reaction mix consisted of 0.5μl positive and negative primers (10 mol/l each), 10 μl PCR master mix, 2 μl template, and DEPC water to achieve the final volume. The following temperature cycling conditions were used: 95°C for 30 s, 40 cycles of 95°C for 5 s, and 60°C for 32 s. Real-time PCR amplification was performed using the ABI 7500 Real-time PCR Detection System (Foster City, CA). Primer 3.0 software was used to design the primers (http://Frodo.wi.mit.edu). The sequences of the primers were shown in Table 2.

Western blotting. Cell or tissue lysates were prepared using radioimmunoprecipitation

assay (RIPA) buffer containing a protease inhibitor cocktail (Roche) and a phosphatase inhibitor. Immunoblotting was performed with primary antibodies against FN1 (1:1000), Collagen I (1:500), Collagen III (1:500), α-SMA (1:1000), BMP1 (1:1000) and GAPDH (1:1000) followed by the addition of HRP-labeled secondary antibodies. The blots were visualized using the Amersham Biosciences ECL detection system (Amersham, Little Chalfont, UK). Densitometric analysis was performed using Quantity One software (Bio-Rad).

Cell proliferation and cytotoxicity assay. mPTCs and NRK-49F were seeded in a 96-well plate at a density of 10^4-10^5 cells/well in 100 μL of culture medium and cultured in a CO2 incubator at 37°C for 24 hours. Then various concentrations of UK383,367 (0-1000nM) was added to the wells. After 24h incubation in the incubator, 10 μL of CCK-8 solution was added to each well of the plate followed by the incubation in incubator for 1-4 hours. The absorbance at 450 nm was measured using a microplate reader.

Kidney histopathological analysis. Kidney tissues were fixed with 4% paraformaldehyde, embedded in paraffin, and sectioned transversely. Kidney sections (3 μm) were stained with Masson staining.

Immunohistochemical analysis. Kidneys were fixed in 4% paraformaldehyde and embedded in paraffin. Paraffin sections of each specimen were cut at a thickness of 3 μm, and a standard protocol, using xylene and graded ethanol, was employed to deparaffinize and rehydrate the tissue. These sections were washed with PBS and treated with blocking buffer containing 50 mM NH4Cl, 2% BSA, and 0.05% saponin

in PBS for 20 min at room temperature. The sections were then incubated overnight at 4°C with Collagen I (1:250), Collagen III (1:200), BMP1 (1:200) or MCP1 (1:250) antibodies. After washing with PBS, the secondary antibody was applied, and the signals were visualized using an ABC kit (Santa Cruz Biotechnology).

IL-1β concentration analysis. Serum IL-1β expression levels were determined using enzyme-linked immunosorbent assay (ELISA) kits according to the provided instructions. Samples were run in duplicate, and the results were averaged for all assays.

Renal function evaluation. Serum, urine creatinine and BUN concentrations of mice were analyzed in the central laboratory of our hospital. Creatinine clearance was calculated according to the formula: urine creatinine (μmol/L) × 24h urine volume (ml)/ serum creatinine (μmol/L) ×1000/ weight (g) × [1/1440]. Albuminuria was determined by ELISA Kit (Bethyl, Hamburg, Germany) according to the manufacturers' instructions.

Blood pressure measurement. The systolic blood pressure of the mice was measured by Tail-cuff method, sing a Visitech BP2000 Blood Pressure Analysis System (Apex, NC).

Statistical analysis. All data are presented as the means ± standard error of mean (SEM). Differences between 2 groups were analyzed using two-tailed Student's t-test and incorporated into GraphPad Prism 6 software (GraphPad Software). ANOVA was used for comparisons among multiple groups. $P < 0.05$ was considered significant.

RESULTS

BMP1 expression in fibrotic kidneys from CKD patients and UUO mice. We examined BMP1 expression by means of immunohistochemistry and Western blotting. As shown in Fig. 1A, compared with the normal kidney tissue, BMP1 protein expression showed striking upregulation in renal tubules and tubulointerstitial region. In UUO mice, expression of BMP1 protein was similarly enhanced in obstructive kidney (Fig. 1B), which was further confirmed by Western blotting analysis (Fig. 1 C and D). Above data suggested a possible role of BMP1 in the pathogenesis of renal fibrosis.

UK383,367 improved renal pathology in obstructive kidneys from UUO mice. In order to define the role of BMP1 in renal pathology in CKD, we treated UUO mice with BMP1 inhibitor UK383,367. As shown by Masson's trichrome staining, the substantial accumulation of collagen fibrils in the interstitium of obstructive kidneys was remarkably attenuated by UK383,367 (Fig. 2A and B).

UK383,367 suppressed renal interstitial fibrosis induced by UUO. Next, we further examined the expression of collagen I and collagen III by immunohistochemistry and observed that the deposition of collagen I and collagen III was significantly induced in the tubulointerstitium of the UUO mice, compared with the sham group. UK383,367 treatment markedly blunted the deposition of these collagens (Fig. 3A and B). In agreement with the immunostaining data, qRT-PCR and Western blotting analyses further confirmed the downregulation of collagen I, collagen III in line with the decreased FN and α-SMA after UK383,367 treatment (Fig. 3C-E). These results

provided more solid evidence indicating that UK383,367 could suppress renal interstitial fibrosis induced by UUO.

UK383,367 suppressed renal inflammation induced by UUO. Inflammation in kidney is a feature of CKD. Thus, we also evaluated the inflammatory status in obstructive kidneys with or without UK383,367 treatment. As expected, we found that the enhanced mRNA and protein expression of IL-1β was significantly blunted along with a trend blockade of MCP1 after UK383,367 treatment (Fig. 4A-C). By immunostaining, we also observed a reduction of MCP1 in obstructive kidneys after UK383,367 therapy (Fig. 4D). These results indicated that UK383,367 could ameliorate renal inflammation in UUO.

UK383,367 had no effect on blood pressure and renal function. In order to define the effect of UK383,367 on mice under normal condition, we treated C57BL/6J male mice with UK383,367 for 8 days and found that UK383,367 had no effect on blood pressure (BP), serum creatinine , BUN, creatinine clearance, albuminuria, and tubular injury in histology (Figure 5A-F).

UK383,367 reduced TGF-β1-induced profibrotic response in mPTCs. To detect the direct effect of UK383,367 on profibrotic response in kidney cells, UK383,367 was added to mouse renal tubular epithelial cells stimulated by TGF-β1. By a CCK8 assay, we detected cell viability with different concentrations of UK383,367 (Fig. 6A) and determined 200 nM as a suitable concentration used in following experiments of mPTCs. As shown by the data from qRT-PCR and Western blots, UK383,367 treatment could significantly inhibit the synthesis of collagen I, collagen III, and FN

and the upregulation of α-SMA (Fig. 6B-D). These data indicated a direct inhibitory effect of UK383,367 on the production of extracellular matrix and cell phenotype transition.

UK383,367 blocked TGF-β1-induced activation of NRK-49F cells. Finally, we also detected the action of UK383,367 in the activation of NRK-49F cells (a cell line of renal fibroblasts) stimulated by TGF-β1. As shown in Fig. 7A, by a CCK8 assay, we detected cell viability with different concentrations of UK383,367 and determined 100 nM and 200 nM as suitable concentrations used in following experiments of NRK-49F cells. UK383,367 administration obviously blocked the activation of renal fibroblasts of NRK-49F cells (Fig. 7B and C). These data further indicated an anti-fibrotic role of UK383,367 possibly through inactivating the activation of renal fibroblasts.

BMP1 promoted TGF-β1-induced profibrotic response in mPTCs. Since the BMP1 inhibitor UK383,367 was anti-fibrotic, we further explored the effect of BMP1 on profibrotic response in mPTCs. As shown in Fig. 8, overexpression of BMP1 significantly aggravated TGF-β1-induced expressions of FN, collagen I and α-SMA. These data indicated BMP1 could accelerate TGF-β1-induced profibrotic response.

DISCUSSION

Renal fibrosis is a poor prognostic indicator of CKD, leading to the progression to ESRD (16). In the present study, employing animals and cells, we investigated the contribution of UK383,367, a procollagen C-proteinase inhibitor, in the development

of renal fibrosis in CKD. To our knowledge, the current study is the first one to examine UK383,367 effect on renal fibrosis. The findings indicated that UK383,367 strikingly attenuated renal fibrosis in vivo and in vitro.

Although the underlying molecular mechanism of renal fibrosis is still elusive, the imbalance of the synthesis and degradation of the components of ECM could roughly explain the development of renal fibrosis in CKD. This process yields irreversible kidney scarring and subsequent loss of renal function(17). The inhibition of myofibroblast-mediated synthesis of ECM is becoming a potential to develop the antifibrotic therapies in CKD(4, 23). P. V. Fish et al(6) demonstrated that treatment with UK383,367 prevented ECM formation in skin scarring. No report has referred to the role of UK383,367 in renal fibrosis. In this study, we observed that UK383,367 markedly blocked the accumulation of ECM components of collagen I, collagen III, and fibronectin both in UUO model and TGF-β1-treated kidney cells. The corresponding molecular mechanism was that UK383,367 might target BMP1 to inhibit the production of matured collagens.

BMP1 inhibition is considered as a potential method for treating fibrosis because BMP1 is required to convert pro-collagen to collagen. Other researchers have reported that antibody against BMP1 is advantageous for post myocardial infarction recovery, during which fibrotic scarring often occurs in heart(5), and liver fibrosis induced by CCl_4(8), as well as renal fibrosis caused by kidney mass reduction(9). Considering the robust action of BMP1 in antagonizing scar formation, some inhibitory compounds against BMP1 were developed, including UK383,367 (1, 2, 6, 11). Herein, we

demonstrated a protective action of BMP1 inhibitor UK383,367 against renal fibrosis in vivo and in vitro. In this study, we also observed a reduction of the mRNA levels of collagens, FN, and α -SMA following the treatment of UK383,367, which might be a secondary response to ameliorated renal fibrosis.

It is also known that renal fibrosis in CKD is accompanied by the infiltration and activation of different types of inflammatory cells, as well as the secretion of inflammatory factors including chemokine, interleukin, tumor necrosis factor, complement and so on(13). The continuous inflammatory response can form a vicious cycle, leading to the activation of the profibrotic signal pathways and thus promoting the kidney fibrosis(18). On the other hand, fibrotic response could also contribute to the inflammation(20). The data from current study showed that the levels of proinflammatory factors of MCP-1 and IL-1β were significantly reduced in the obstructive kidneys following UK383,367. Such a phenomenon could be explained by a subsequent response to the attenuated renal fibrosis. Certainly, as a compound, we also cannot rule out an off-target effect of UK383,367 in antagonizing inflammation, which needs to be investigated in the future.

In summary, we found that UK383,367 attenuated renal fibrosis and inflammation in CKD. Mechanistically, UK383,367 could interfere with collagens (main components of ECM) deposition by inhibiting BMP1. Our results provided first evidence showing the strong effect of UK383,367 on renal fibrosis in CKD, suggesting that UK383,367 might be a potential drug in the prevention and treatment of renal fibrosis.

GRANTS

This work was supported by grants from National Natural Science Foundation of China (Nos.81700595，81873599, 81570616, 81770690,81670678), the National Key Research and Development Program (no. 2016YFC0906103) and the Natural Science Foundation of Nanjing Medical University (no. NMUB2018372)

DISCLOSUREs

The authors declare no conflicts of interest, financial or otherwise.

AUTHOR CONTRIBUTIONS

M.B., Z.J. and A.Z. designed the experiments. M.B., J.L., S.W., D.D., X.Y., Y.G., S.C., D.L., and Y.D. were responsible for the experiments and data collection. M.B., J.L., D.D. and Y.Z. performed data analysis. M.B., J.L., D.D., X.Y., Y.G., S.C., Y.Z., S.H, Z.J and A.Z. conducted the data interpretation. All the authors contributed to and approved the final manuscript.

REFERENCES

1. **Allan GA, Gedge JI, Nedderman AN, Roffey SJ, Small HF, and Webster R**. Pharmacokinetics and metabolism of UK-383,367 in rats and dogs: a rationale for long-lived plasma radioactivity. *Xenobiotica* 36: 399-418, 2006.

2. **Bailey S, Fish PV, Billotte S, Bordner J, Greiling D, James K, McElroy A, Mills JE, Reed C, and Webster R**. Succinyl hydroxamates as potent and selective non-peptidic inhibitors of procollagen C-proteinase: design, synthesis, and evaluation as topically applied, dermal anti-scarring agents. *Bioorg Med Chem Lett* 18: 6562-6567, 2008.

3. **Bello AK, Levin A, Tonelli M, Okpechi IG, Feehally J, Harris D, Jindal K, Salako BL, Rateb A, Osman MA, Qarni B, Saad S, Lunney M, Wiebe N, Ye F, and Johnson DW**. Assessment of Global Kidney Health Care Status. *JAMA* 317: 1864-1881, 2017.

4. **Chen J, and Li D**. Telbivudine attenuates UUO-induced renal fibrosis via TGF-beta/Smad and

NF-kappaB signaling. *Int Immunopharmacol* 55: 1-8, 2018.

5. **Cvjeticanin B, Prutki M, Dumic-Cule I, Veir Z, Grgurevic L, and Vukicevic S**. Possible target for preventing fibrotic scar formation following acute myocardial infarction. *Med Hypotheses* 83: 656-658, 2014.

6. **Fish PV, Allan GA, Bailey S, Blagg J, Butt R, Collis MG, Greiling D, James K, Kendall J, McElroy A, McCleverty D, Reed C, Webster R, and Whitlock GA**. Potent and selective nonpeptidic inhibitors of procollagen C-proteinase. *J Med Chem* 50: 3442-3456, 2007.

7. **Ge G, and Greenspan DS**. Developmental roles of the BMP1/TLD metalloproteinases. *Birth Defects Res C Embryo Today* 78: 47-68, 2006.

8. **Grgurevic L, Erjavec I, Grgurevic I, Dumic-Cule I, Brkljacic J, Verbanac D, Matijasic M, Paljetak HC, Novak R, Plecko M, Bubic-Spoljar J, Rogic D, Kufner V, Pauk M, Bordukalo-Niksic T, and Vukicevic S**. Systemic inhibition of BMP1-3 decreases progression of CCl4-induced liver fibrosis in rats. *Growth Factors* 35: 201-215, 2017.

9. **Grgurevic L, Macek B, Healy DR, Brault AL, Erjavec I, Cipcic A, Grgurevic I, Rogic D, Galesic K, Brkljacic J, Stern-Padovan R, Paralkar VM, and Vukicevic S**. Circulating bone morphogenetic protein 1-3 isoform increases renal fibrosis. *Journal of the American Society of Nephrology : JASN* 22: 681-692, 2011.

10. **Hopkins DR, Keles S, and Greenspan DS**. The bone morphogenetic protein 1/Tolloid-like metalloproteinases. *Matrix Biol* 26: 508-523, 2007.

11. **Kallander LS, Washburn D, Hilfiker MA, Eidam HS, Lawhorn BG, Prendergast J, Fox R, Dowdell S, Manns S, Hoang T, Zhao S, Ye G, Hammond M, Holt DA, Roethke T, Hong X, Reid RA, Gampe R, Zhang H, Diaz E, Rendina AR, Quinn AM, and Willette B**. Reverse Hydroxamate Inhibitors of Bone Morphogenetic Protein 1. *ACS Med Chem Lett* 9: 736-740, 2018.

12. **Kessler E, Takahara K, Biniaminov L, Brusel M, and Greenspan DS**. Bone morphogenetic protein-1: the type I procollagen C-proteinase. *Science* 271: 360-362, 1996.

13. **Klahr S, and Morrissey J**. Obstructive nephropathy and renal fibrosis. *American journal of physiology Renal physiology* 283: F861-875, 2002.

14. **Levin A, Tonelli M, Bonventre J, Coresh J, Donner JA, Fogo AB, Fox CS, Gansevoort RT, Heerspink HJL, Jardine M, Kasiske B, Kottgen A, Kretzler M, Levey AS, Luyckx VA, Mehta R, Moe O, Obrador G, Pannu N, Parikh CR, Perkovic V, Pollock C, Stenvinkel P, Tuttle KR, Wheeler DC, Eckardt KU, and participants ISNGKHS**. Global kidney health 2017 and beyond: a roadmap for closing gaps in care, research, and policy. *Lancet* 2017.

15. **Li SW, Sieron AL, Fertala A, Hojima Y, Arnold WV, and Prockop DJ**. The C-proteinase that processes procollagens to fibrillar collagens is identical to the protein previously identified as bone morphogenic protein-1. *Proceedings of the National Academy of Sciences of the United States of America* 93: 5127-5130, 1996.

16. **Liu Y**. Cellular and molecular mechanisms of renal fibrosis. *Nature reviews Nephrology* 7: 684-696, 2011.

17. **Nogueira A, Pires MJ, and Oliveira PA**. Pathophysiological Mechanisms of Renal Fibrosis: A Review of Animal Models and Therapeutic Strategies. *In Vivo* 31: 1-22, 2017.

18. **Noronha IL, Fujihara CK, and Zatz R**. The inflammatory component in progressive renal disease--are interventions possible? *Nephrology, dialysis, transplantation : official publication of the European Dialysis and Transplant Association - European Renal Association* 17: 363-368, 2002.

19. **Tabas JA, Zasloff M, Wasmuth JJ, Emanuel BS, Altherr MR, McPherson JD, Wozney JM,**

and Kaplan FS. Bone morphogenetic protein: chromosomal localization of human genes for BMP1, BMP2A, and BMP3. *Genomics* 9: 283-289, 1991.

20. **Tang PM, Nikolic-Paterson DJ, and Lan HY**. Macrophages: versatile players in renal inflammation and fibrosis. *Nature reviews Nephrology* 15: 144-158, 2019.

21. **Webster AC, Nagler EV, Morton RL, and Masson P**. Chronic Kidney Disease. *Lancet* 389: 1238-1252, 2017.

22. **Yamaguchi J, Tanaka T, and Nangaku M**. Recent advances in understanding of chronic kidney disease. *F1000Research* 4: 2015.

23. **Zeisberg M, and Kalluri R**. Cellular mechanisms of tissue fibrosis. 1. Common and organ-specific mechanisms associated with tissue fibrosis. *Am J Physiol Cell Physiol* 304: C216-225, 2013.

Table 1. The basic information and diagnosis of CKD patients

Gender	Age (yr)	Proteinuria (g/24 h)	Pathological diagnosis	Serum Creatine (μmol/L)	BUN (mmol/ L)
Boy	6.7	3.56	FSGS	382	9.95
Girl	7.8	0.31	DIN	1111	55.10
Boy	10.2	4.38	IgA nephropathy	46	3.18
Girl	2.8	1.41	DIN	428	23.17
Boy	10.0	1.95	Sclerosing glomerulonephritis	630	41.80
Girl	2.0	0.22	FSGS	41	4.73
Boy	3.8	2.07	Sclerosing glomerulonephritis	58	6.03
Boy	10.9	4.59	IgA nephropathy	106	6.55

425

426 **Table 2. The sequences of the primers used in the study.**

Primer Name	Primer Sequence 5′ -3′
FN1-F	ATGTGGACCCCTCCTGATAGT
FN1-R	GCCCAGTGATTTCAGCAAAGG
TGF-β1-F	CTCCCGTGGCTTCTAGTGC
TGF-β1-R	GCCTTAGTTTGGACAGGATCTG
α -SMA-F	CCCAGACATCAGGGAGTAATGG
α-SMA-R	TCTATCGGATACTTCAGCGTCA
Collagen I-F	TAAGGGTCCCCAATGGTGAGA
Collagen I-R	GGGTCCCTCGACTCCTACAT
Collagen III-F	CAGGACCTAAGGGCGAAGATG
Collagen III-R	TCCGGGCATACCCCGTATC
GAPDH-F	AATGGATTTGGACGCATTGGT
GAPDH-R	TTTGCACTGGTACGTGTTGAT
BMP1-F	TTGTACGCGAGAACATACAGC
BMP1-R	CTGAGTCGGGTCCTTTGGC

427

428 **Figure Legends**

429 Fig. 1. BMP1 expression in fibrotic kidneys from CKD patients and UUO mice. (A &
430 B) Representative immunohistochemical staining of BMP1 in children with CKD
431 (n=8) and UUO mice (n=4). Normal renal tissues were collected from patients
432 without proteinuria who received a partial nephrectomy of a benign renal tumor (n=6).
433 (C) Western blots analyses of BMP1 in kidneys of UUO mice. GAPDH was used as
434 loading control (n=4). (D) Semiquantitative analysis of average optical density of
435 BMP1. The values represent means ± SEM. For the control group vs. CKD group, the
436 UUO group vs. the sham group, *indicates $P < 0.05$.

Fig. 2. UK383,367 ameliorated histologic changes induced by UUO. (A) Deposition of total fibrosis in kidney tissues was determined by Masson's trichrome staining (×200). (B) The relative fibrotic area (%), based on Masson's trichrome staining. Scale bar, 50 μm. The values represent means ± SEM (n=7 per group). For the UUO group vs. the sham group, *indicates $P < 0.05$. For the UK-treated group vs. the UUO group, # indicates $P < 0.05$.

Fig. 3. UK383,367 reduced renal interstitial fibrosis in UUO animals. (A & B) Immunohistochemical staining of collagen I and III (×200). Scale bar, 50 μm. (C) qPCR analysis of FN1, Collagen I, Collagen III and α-SMA (n=7 per group). (D) Western blot of FN1, Collagen I, Collagen III and α-SMA (n=7 per group). (E) Semiquantitative analysis of average optical density of FN1, Collagen I, Collagen III and α-SMA. The values represent means ± SEM. For the UUO group vs the sham group, *indicates $P < 0.05$. For the UK-treated group vs the UUO group, # indicates $P < 0.05$.

Fig. 4. UK383,367 ameliorated renal inflammation in UUO animals. (A and B) qPCR analysis of MCP-1 and IL-1β. (C) ELISA analysis of IL-1β in serum. (D) Representative immunohistochemical staining of MCP1. The values represent means ± SEM (n=7 per group). For the UUO group vs the sham group, *indicates $P < 0.05$. For the UK-treated group vs the UUO group, # indicates $P < 0.05$.

Fig. 5. UK383,367 had no effect on blood pressure and renal function. C57BL/6J male mice were treated with UK383,367 for 8 days. (A) Continuous measurement of blood pressure (BP) for 8 days. (B-F) Analysis of serum creatinine(B), BUN (C),

creatinine clearance (D), albuminuria (E), and PAS staining (F). The values represent means ± SEM (n=8 per group).

Fig. 6. UK383,367 suppressed TGF-β1-induced fibrotic response in mPTCs. (A) Analysis of cell viability by CCK8. mPTCs were treated with different concentrations of UK383,367 (n=7-10 per group). (B) qPCR analysis of FN1, Collagen I and α-SMA (n=5 per group). (C) Western blots of FN1, Collagen I, Collagen III and α-SMA. (D) Semiquantitative analysis of average optical density of FN1, Collagen I, Collagen III and α-SMA (n=3 per group). mPTCs were pre-treated UK383,367 (200nM) for half an hour, then treated with TGF-β1 (10ng/ml) for 24h. The values represent means ± SEM. For the TGF-β1 group vs the control group, *indicates $P < 0.05$. For the UK-treated group vs the TGF-β1 group, # indicates $P < 0.05$.

Fig. 7. UK383,367 inhibited TGF-β1-induced fibrotic response in NRK-49F cells. (A) Analysis of cell viability by CCK8. NRK-49F cells were treated with different concentrations of UK383,367 (n=7-10 per group). (B) Western blot of FN1, Collagen I and α-SMA. (C) Semiquantitative analysis of average optical density of FN1, Collagen I and α-SMA. In B & C, NRK-49F cells were pre-treated UK383,367 (100nM, 200nM) for half an hour, then treated with TGF-β1 (10ng/ml) for 24h. The values represent means ± SEM (n=3 per group). For the TGF-β1 group vs the control group, *indicates $P < 0.05$. For the UK-treated group vs the TGF-β1 group, # indicates $P < 0.05$.

Fig. 8. BMP1 promoted TGF-β1-induced profibrotic response in mPTCs. mPTCs cells were transfected with BMP1 plasmids for 24h, then treated with TGF-β1

481 (10ng/ml) for another 24h. (A-D) qPCR analysis of BMP1 (A), FN1 (B), Collagen I
482 (C), and α-SMA (D). The values represent means ± SEM (n=4 per group). For the
483 BMP1 group vs the control group, *indicates $P < 0.05$.
484

Figure 1

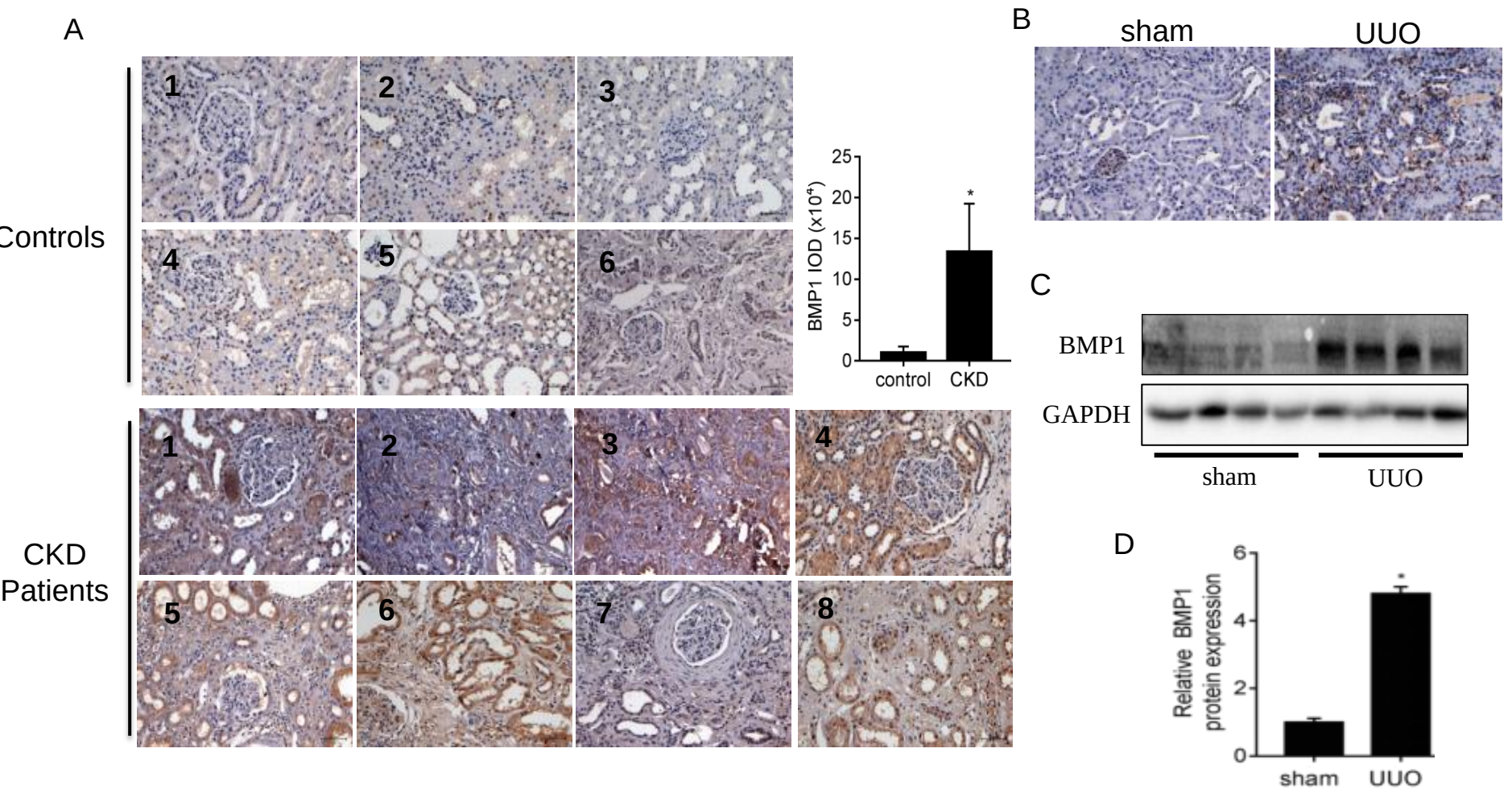

Figure 2

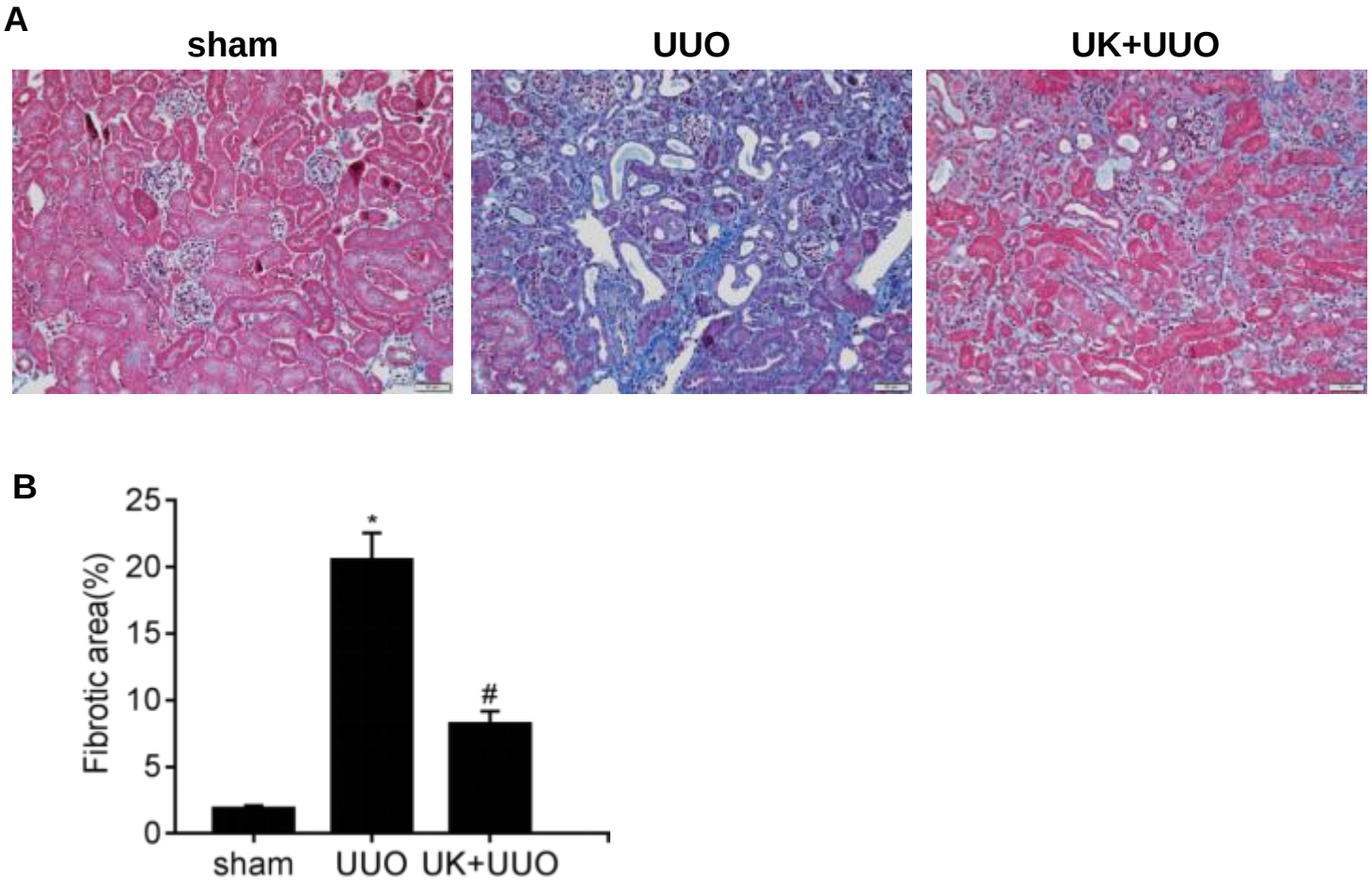

Figure 3

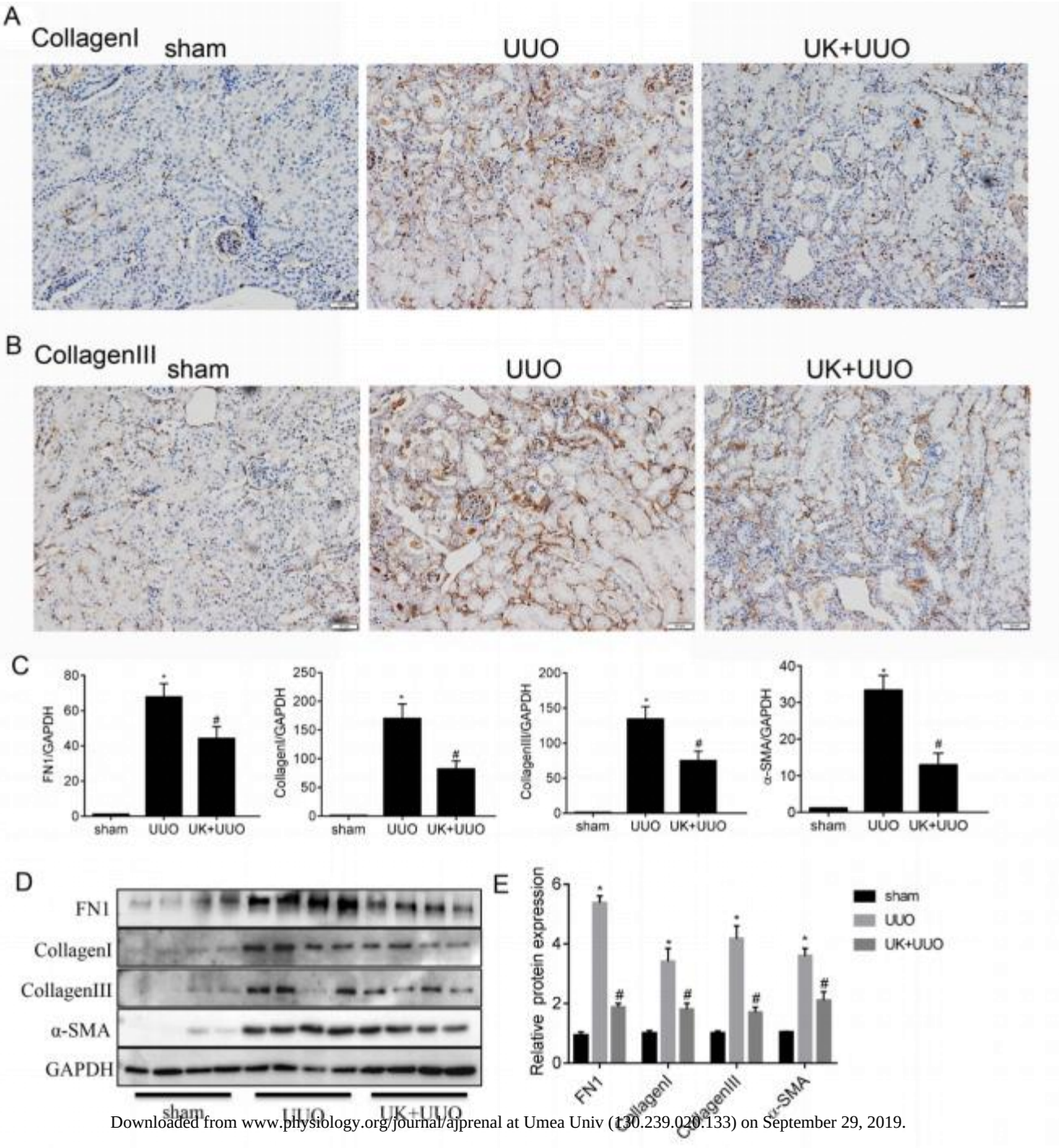

Figure 4

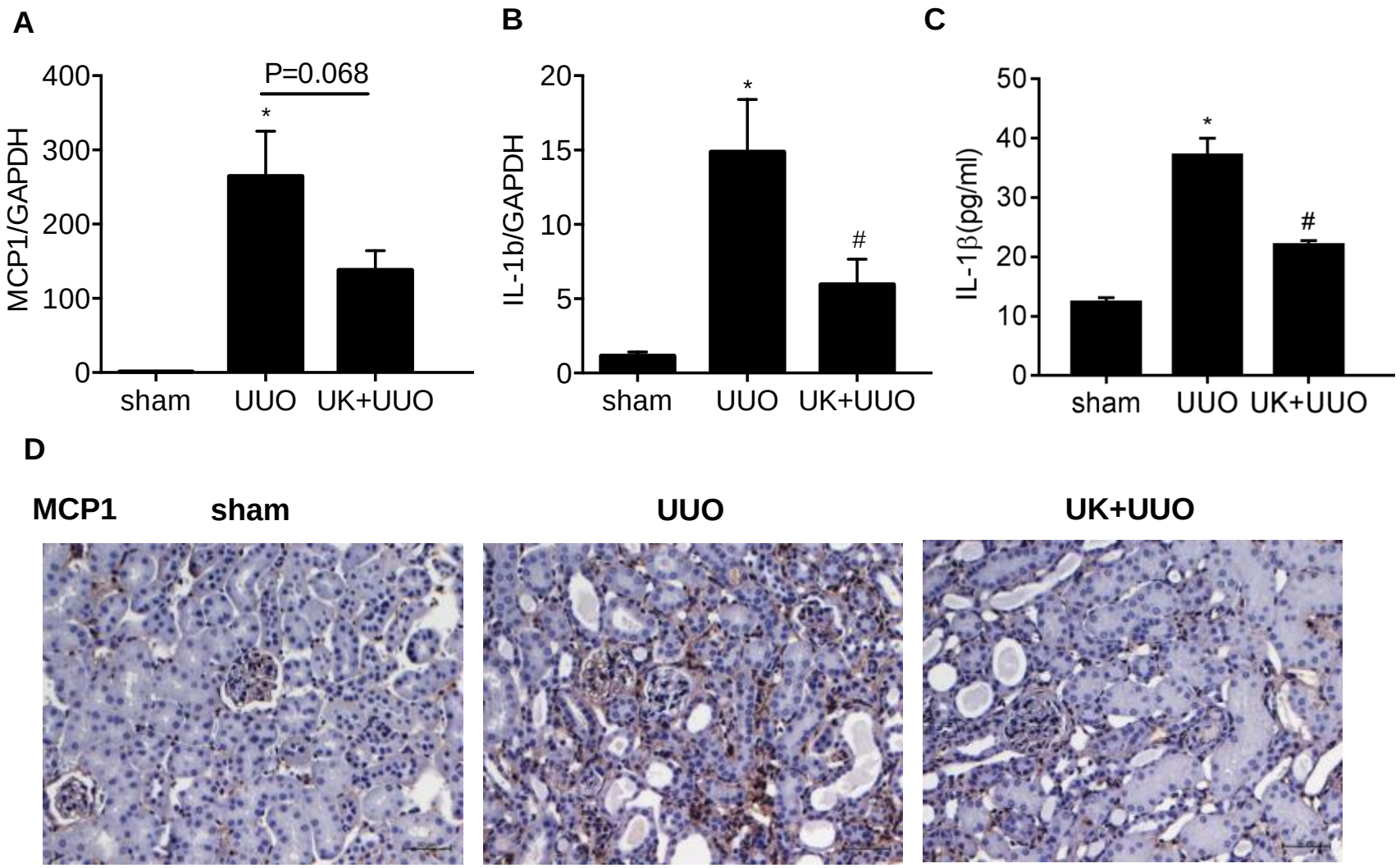

Figure 5

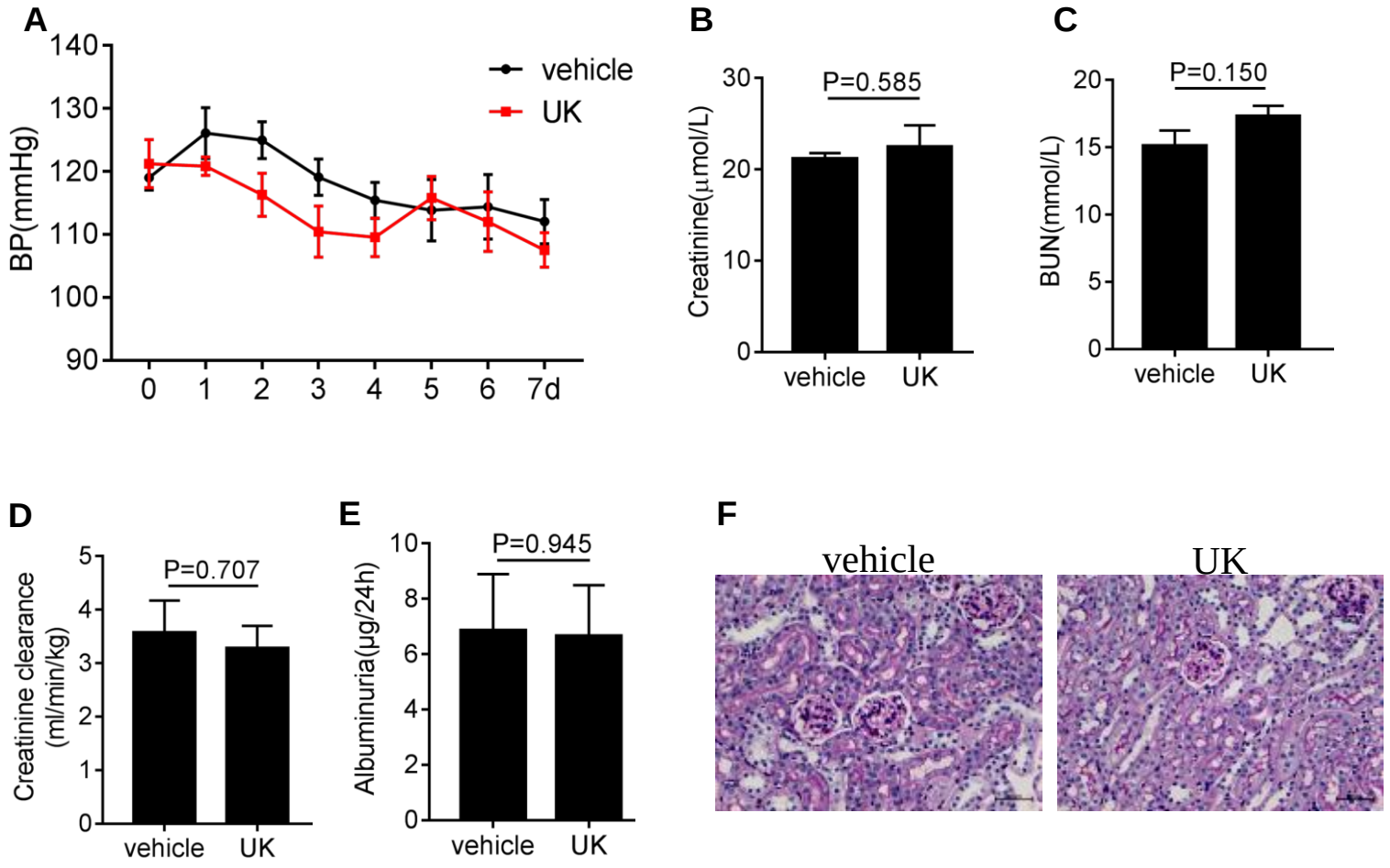

Figure 6

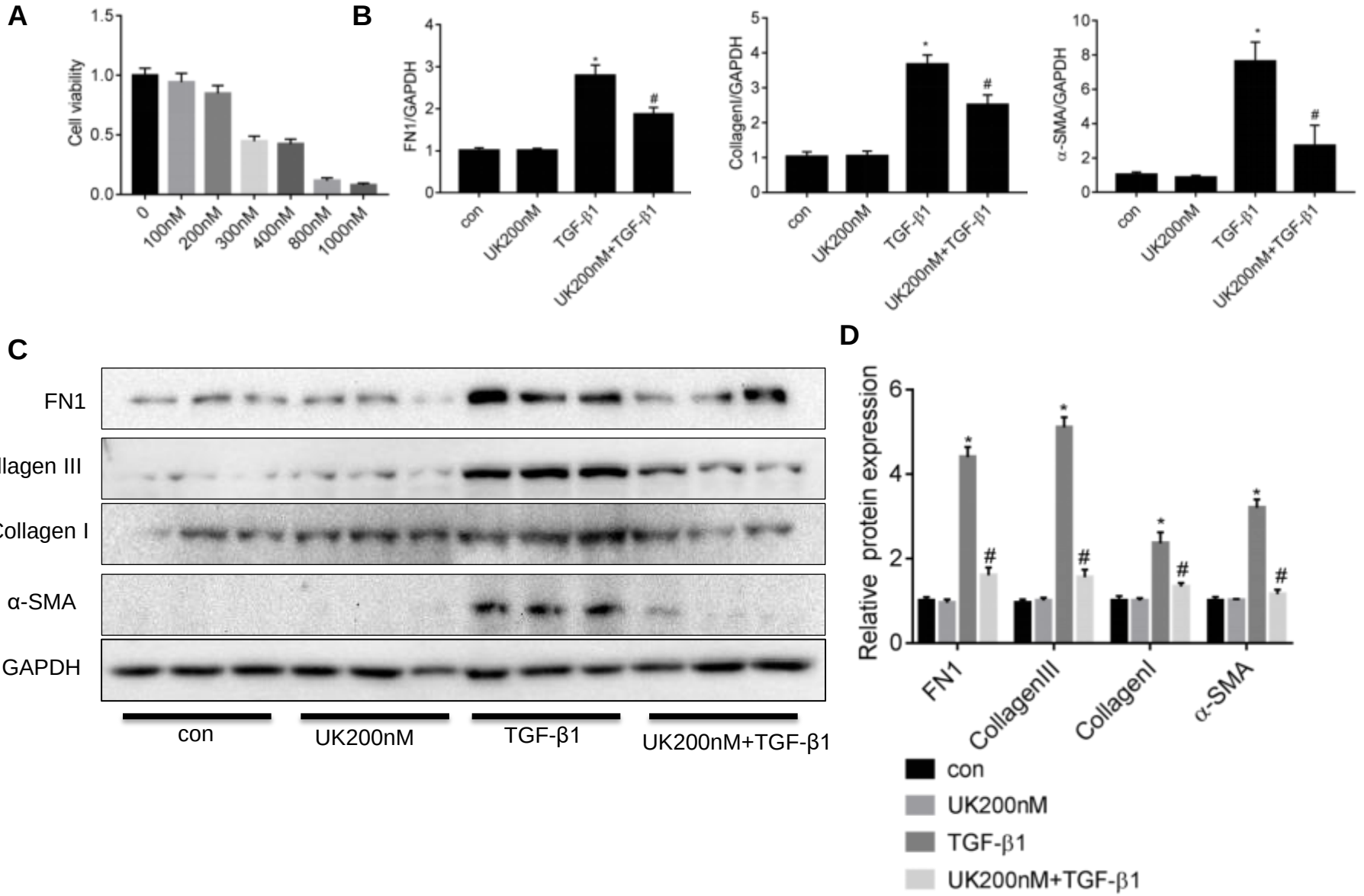

Figure 7

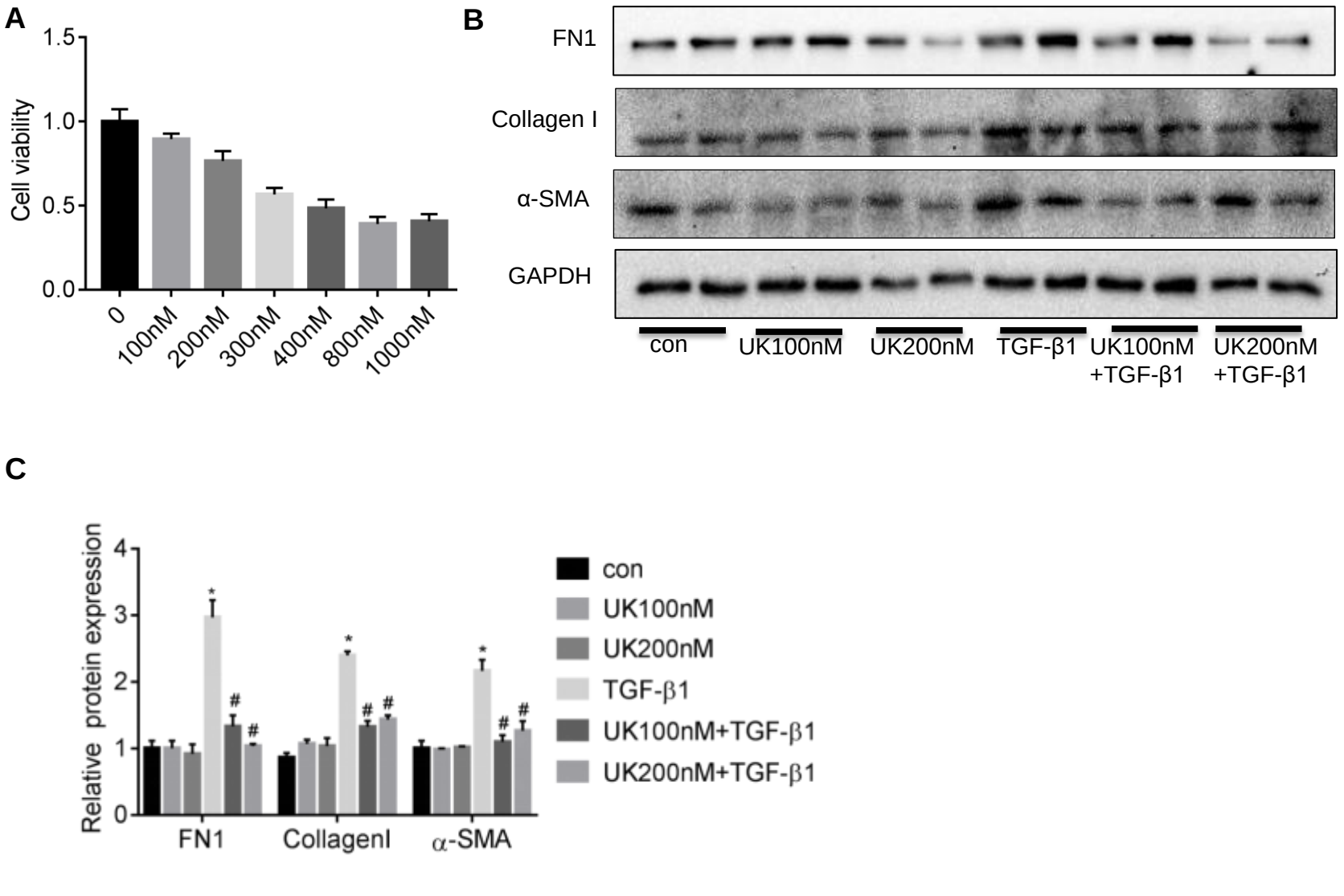

Figure 8